Ocean Sci. Discuss., https://doi.org/10.5194/os-2018-78
Manuscript under review for journal Ocean Sci.
Discussion started: 10 September 2018

Ocean Science
Discussions
Open Access
EGU

Influence of hydrodynamic mixing on the distribution of dissolved organic carbon in the East China Sea and the northwest Pacific

Ling Ding[1], Tiantian Ge[1] and Xuchen Wang[1,2,*]

[1]Key Laboratory of Marine Chemistry Theory and Technology, Ministry of Education, Ocean University of China, Qingdao, 266100, China

[2] Center for Isotope Geochemistry and Geochronology, Qingdao National Laboratory for Marine Science and Technology, Qingdao, 266061, China

[*]**Correspondence:** Xuchen Wang (xuchenwang@ouc.edu.cn)

Abstract. Oceanic dissolved organic carbon (DOC) is one of the largest carbon reservoirs on Earth, and its distribution and behavior play important roles in carbon cycling and biogeochemical processes in the ocean. Here, we report distribution and concentrations of DOC for water samples collected from the shelf-edge and slope regions in East China Sea (ECS) and the Kuroshio Extension (KE) in the northwestern North Pacific (NP) during two cruises in 2014-2015. Concentrations of DOC were 45-88 μM in the ECS and 35-65 μM in the KE. In addition to biological processes, the distribution of DOC is largely controlled by hydrodynamic mixing of different water masses. The intrusion of Kuroshio Current could dilute DOC concentrations at stations in the outer shelf and slope ranges of the ECS. The inverse correlation of DOC with apparent oxygen utilization (AOU) suggests that DOC oxidation only contributes 18% of the oxygen consumption in the ECS slope waters. In contrast, concentrations of DOC

Ocean Sci. Discuss., https://doi.org/10.5194/os-2018-78
Manuscript under review for journal Ocean Sci.
Discussion started: 10 September 2018

in the KE were significantly lower in surface waters, and a relatively low and stable DOC level (~ 40 μM) was found in deep waters. The observed spatial variations of DOC in the upper 700 m among the stations in the KE were largely influenced by the mixing of the two water masses carried by the two major western boundary currents: Kuroshio and Oyashio that mix and form the KE. The hydrodynamic processes play important roles not only in the distribution of DOC but nutrients as well, thus could have major impact to primary production and ecosystems in the KE region.

1 Introduction

The world's oceans contain the largest reservoir of carbon on earth, and dissolved organic carbon (DOC) is the largest active reduced carbon pool (685 Pg C) in the ocean (Hansell and Carlson, 1998; Hansell et al., 2009). DOC is a highly diverse organic molecular mixture in which ~ 20,000 individual compounds have been detected (Riedel and Dittmar, 2014). Its concentration and distribution therefore play significant roles not only in the global carbon cycle, but also in controlling and regulating the microbial community and many biogeochemical processes in the oceans (Azam et al., 1983; Fenchel, 2008; Carlson et al., 2010; Nelson and Carlson, 2012). Since DOC in the ocean is directly linked to the oceanic dissolved inorganic carbon (DIC) system through biological processes, the DOC pool in the ocean also indirectly contributes to the sink of atmospheric CO_2 (Druffel et al., 1992; Carlson et al., 1994; Carlson et al., 1998; Hansell and Carlson, 2001; Carlson et al., 2010).

In the last 20 years, improved precision of DOC concentration analysis via the high-temperature catalytic oxidation (HTCO) technique has revealed detailed oceanic DOC distributions, such as those generated by the US Climate Variability Repeat (CLIVAR) Hydrography program (Sharp et al., 1995; Sharp et al., 2002; Carlson et al., 2010; Hansell et al., 2012; Bercovici and Hansell, 2016). In general, physical and biological processes combine

Ocean Sci. Discuss., https://doi.org/10.5194/os-2018-78
Manuscript under review for journal Ocean Sci.
Discussion started: 10 September 2018

in modulating the distribution and dynamics of DOC in open oceans (Hansell and Waterhouse, 1997; Ogawa et al., 1999; Hansell et al., 2009; Carlson et al., 2010; Bercovici and Hansell, 2016). It has been widely observed that oceanic DOC accumulates in the upper water column (100 m) at elevated concentrations (70-90 μM) compared to its relatively constant values (35-45 μM) in deep water (>1000 m), reflecting biological production of DOC in the euphotic zone and microbial consumption with depth (Hansell et al., 2009). In the upper ocean, DOC distribution displays obvious latitudinal patterns with relatively higher concentrations (65-85 μM) in the subtropical ocean above 100 m, where stratification may restrict vertical water mixing (Abell et al., 2000; Carlson et al., 2010; Pan et al., 2014). However, in high latitude areas, DOC concentrations remain at relatively low levels (45-60 μM) as a result of deep water penetration that dilutes DOC concentrations (Ogawa et al., 1999; Abell et al., 2000; Pan et al., 2014). In the deep ocean, about a 14 μM decrease in DOC concentrations was seen along the abyssal circulation pathway from the North Atlantic to the North Pacific Ocean, due to differences in thermohaline circulation patterns (Hansell and Carlson, 1998). Carlson et al. (2010) later confirmed the DOC export by the Atlantic Ocean's meridional overturning circulation. In addition, concentrations of DOC in the deep Southern Ocean were similar to that in the North Atlantic Deep Water (NADW) but higher than in Pacific deep water, which could result from conservative mixing of ocean deep waters such as the Atlantic, Indian and Pacific (Bercovici and Hansell, 2016).

The northwestern North Pacific (NP) is a very special oceanic region where carbon cycling and biogeochemical processes are greatly influenced by two major oceanic western boundary currents: Kuroshio Current (KC) and Oyashio Current (OC). As one of the largest marginal seas connected to the northwestern NP, the hydrological characteristics of the East China Sea (ECS) are largely influenced by the vigorous exchange between the warm saline Kuroshio and cold fresh continental shelf water masses (Hsueh, 2000). Ogawa et al. (2003) reported that the

Ocean Sci. Discuss., https://doi.org/10.5194/os-2018-78
Manuscript under review for journal Ocean Sci.
Discussion started: 10 September 2018

distribution of DOC was mainly controlled by hydrological rather than by biological processes around the shelf-edge of the ECS. After existing the ECS at 30° N, 128-129° E, the Kuroshio Current flows northeastward and merges with the southward-flowing Oyashio Current in the mixed water region off the coast of Japan, and finally form the Kuroshio Extension (KE) flowing eastward into the North Central Pacific (NCP) (Yasuda et al., 1996; Talley, 1997; Qiu, 2001). The newly-formed North Pacific Intermediate Water (NPIW) in the mixed water region has been given attention, not only its important role in the ocean circulation systems, but also in the regional carbon cycle and climate variability (Talley, 1993; Hansell et al., 2002; Yasuda, 2003; Wu et al., 2012; Hu et al., 2015). However, few studies focused on the distribution and dynamics of DOC around the KE region. DOC analysis from different NP stations revealed the export of DOC accompanied with the NPIW formation and thus reduce the very old DOC ^{14}C-age in the Pacific Ocean interior, but vertical profiles of DOC were only determined at stations in the subpolar water in the northwestern NP (Hansell et al., 2002). DOC observations on WOCE (World Ocean Circulation Experiment) and CLIVAR cruises have collected at P02-Line stations along the 30° N transection, whereas the distribution of DOC near the KE was not investigated during these cruises.

Overall, our understanding of DOC dynamics and cycling in the outer shelf and slope ranges of the ECS and KE region in the northwestern North Pacific is still limited, despite the previous a few studies. We presented the results of DOC concentrations in the ECS and Kuroshio Extension (KE) region in the northwestern NP, and combined them with the observations of dissolved inorganic carbon (DIC) concentrations and dissolved inorganic radiocarbon (Δ^{14}C-DIC) values, to evaluate the roles of physical mixing process on the distribution of DOC in these dynamic ocean regions.

2 Methods

2.1 Study areas

Ocean Sci. Discuss., https://doi.org/10.5194/os-2018-78
Manuscript under review for journal Ocean Sci.
Discussion started: 10 September 2018

104 Water samples were mainly collected from two oceanic regions: the ECS and the KE region
105 in the northwestern NP (Fig. 1). The ECS is one of the largest marginal seas in the northwest
106 NP, with a broad continental shelf area of about 0.5×10^6 km^2 (Gong et al., 2003). In the
107 relatively shallow (< 60 m) and wider inner shelf region, oceanic processes are largely
108 influenced by the inputs of the Yangtze and Yellow Rivers, which are the largest and second
109 largest rivers in China, together delivering a huge amount of terrestrial organic matter into the
110 ECS (Wang et al., 2012; Xu et al., 2016). In the outer shelf and slope region of the ECS, it is
111 affected largely by the northward-flowing Kuroshio Current which impinges on the shelf break
112 and a branch enters the ECS (Chen and Wang, 1999; Guo et al., 2006; Hu et al., 2015; Ge et al.,
113 2016). The higher primary productivity and intersection of different water masses make the
114 ECS a complex region for studying the ocean carbon biogeochemical cycle.
115 The Kuroshio Extension (KE) in the northwestern NP is an important, highly dynamics
116 region where is largely influenced by Kuroshio and Oyashio currents. The Kuroshio Current
117 which carries relatively warm and saline waters flows northward along the east coast of Japan
118 and turns eastward at about 34° N, 140° E, then flows as the KE into the North Central Pacific
119 (Yasuda et al., 1996; Qiu and Chen, 2011). The southward-flowing Oyashio Current which
120 carries fresh and cold subarctic water meets with Kuroshio water at about 37° N and forms the
121 Kuroshio-Oyashio inter-frontal zone where the subarctic water mass mixes with the KE water
122 and flows eastward (Yasuda et al., 1996; Qiu and Chen, 2011; Hu et al., 2015). The new NPIW
123 is formed in the same region, and this is a mixture of relatively fresh, recently ventilated
124 Oyashio water and high salinity Kuroshio water (Yasuda et al., 1996; Talley, 1997; Qiu and
125 Chen, 2011). The mixed water region in the KE has been characterized as an important sink of
126 anthropogenic CO_2 in the northwestern NP (Tsunogai et al., 1993), and it is a key area for
127 understanding regional climate and ecosystem variations, and biogeochemical cycles (Yasuda,
128 2003; Wu et al., 2012; Hu et al., 2015; Nishibe et al., 2017).

Ocean Sci. Discuss., https://doi.org/10.5194/os-2018-78
Manuscript under review for journal Ocean Sci.
Discussion started: 10 September 2018

129

130 **Table 1.** Summary of sampling stations and times in the East China Sea (ECS) and the Kuroshio
131 Extension (KE) in the northwestern North Pacific (NP).

Station #	Latitude (°N)	Longitude (°E)	Depth (m)	Sampling Date
ECS				
Stn.1	28.37	126.69	177	12 July 2014
Stn.7	28.30	126.83	265	
Stn.11	28.43	126.53	148	13 July 2014
Z1	28.07	127.13	1078	
Z2	27.93	127.36	1326	14 July 2014
Z4	28.63	127.00	425	
Z3	27.75	126.63	1415	15 July 2014
KE in NP				
K2	25.10	134.02	4100	5 April 2015
B2	37.00	147.00	5586	27 April 2015
B8	30.97	146.99	6000	11-12 April 2015
B9	29.86	146.53	5500	10-11 April 2015
A1-b	32.63	145.95	4800	18 April 2015
A4	34.00	147.80	5800	25 April 2015
A6	34.02	150.04	5800	23 April 2015
A8	34.04	152.02	5500	21 April 2015

132

133 **2.2 Sample collection**

134 Water samples for DOC analysis were collected from 7 stations on the shelf-edge and slope
135 region of the ECS during a cruise in July 2014 onboard the Japanese *R/V Shinset Maru*, and
136 from 8 deep stations in the KE region and western NP during a cruise in April-May 2015
137 onboard the Chinese *R/V Dongfanghong-2* (Fig. 1). General information about the sampling
138 stations is summarized in Table 1. All water samples were collected using 12 L Niskin bottles
139 deployed on a rosette with a calibrated SeaBird CTD (model SBE 911) that recorded the
140 temperature and salinity profiles. The accuracy of temperature and salinity is 0.001 ° C and
141 0.001, respectively.

142 After collection, water samples from the Niskin bottle were transferred directly into a 1 L
143 pre-combusted (at 550° C for 4 h) glass bottle after being rinsed three times. The water was

Ocean Sci. Discuss., https://doi.org/10.5194/os-2018-78
Manuscript under review for journal Ocean Sci.
Discussion started: 10 September 2018

144 filtered immediately through 0.7 μM pore size Whatman GF/F filters (prebaked at 550° C for 4
145 h) on board. The filtered water samples were acidified with super-high-purity 85% H_3PO_4
146 (Aladdin®) to pH = 2 and preserved frozen at -20° C until chemical analysis.

147 **2.3 Chemical analysis**

148 Concentrations of DOC were analyzed by the high temperature catalytic oxidation (HTCO)
149 method (Sharp et al., 1995; Sharp et al., 2002) using a Shimadzu TOC-L analyzer equipped
150 with an ASI-V autosampler. Potassium hydrogen phthalate (KHP) dissolved in high purity
151 Milli-Q water was used as DOC standard. The quality assessment for DOC measurements was
152 checked against reference low-carbon water and deep sea water (provided by Dr. Hansell at
153 University of Miami, USA). Instrumental blank was subtracted using high purity Milli-Q water
154 that was analyzed before every five samples (before each sample for the deep seawater station).
155 Average blank of DOC measurement was ≤ 5 μM, and the analytic precisions on triplicate
156 injections were ± 3%, respectively. All samples were analyzed in duplicate and average values
157 were reported.

158 The methods for DIC concentrations and Δ^{14}C-DIC measurements have been described in
159 detail in separated papers for the samples collected during the same cruise (Ge et al., 2016;
160 Ding et al., 2018). Briefly, DIC concentrations were measured using a Shimadzu TOC-L
161 analyzer with the total IC mode. Sodium carbonate and sodium bicarbonate dissolved in Milli-
162 Q water were used as DIC standard, and the concentration values were checked against DIC
163 reference materials (deep sea water) for quality assessment (provided by Dr. Dickson at Scripps
164 Institution of Oceanography). Total blanks was about < 0.15% of seawater DIC concentrations,
165 and the analytic precisions were < 3%. For ^{14}C-DIC measurement, DIC was first extracted as
166 gaseous CO_2 using our modified method with extraction efficiencies > 96% (Ge et al., 2016).
167 The ^{14}C-DIC values were analyzed in the National Ocean Sciences Accelerator Mass
168 Spectrometry (NOSAMS) facility at Woods Hole Oceanographic Institution (WHOI). The

Ocean Sci. Discuss., https://doi.org/10.5194/os-2018-78
Manuscript under review for journal Ocean Sci.
Discussion started: 10 September 2018

purified CO_2 was graphitized for $\Delta^{14}C$ analysis using AMS. $\Delta^{14}C$ values are reported as the modern fraction based on the reference material used (McNichol et al., 1994). The conventional ^{14}C ages (years before present, or yr BP) were calculated following Stuiver and Polach (1977). The total uncertainty is 6‰ or better, tested with a DIC standard (Ge et al., 2016).

In addition to DOC and DIC analyses, dissolved oxygen concentrations for the ECS stations (not measured for the Kuroshio Extension stations) were measured using a Seabird oxygen sensor (SBE43, Sea-Bird Electronics, Inc) with the accuracy of 0.01mL/L. The sensor was pre-calibrated using the concentration that was determined by the Winkler method. The relationship between the Winkler oxygen concentrations and the SBE43 sensor values was evaluated using a regression analysis, we then applied the regression equations to describe the dataset due to the small drift of the dissolved oxygen sensor over the cruise. Finally, apparent oxygen utilization (AOU) was determined by subtracting observed dissolved oxygen concentration from its saturated solubility at *in situ* potential temperature and salinity.

3 Results

3.1 Hydrographic profiles

Hydrographic parameters of the sampling stations (temperature and salinity) recorded with the CTD were summarized in Table S1 in the Supporting information, and the depth profiles were plotted in Fig. 2. Because our study involved two distinctive oceanic regions, we plotted the hydrographic depth profiles for stations in the ECS and KE regions separately.

As shown in Fig. 2a for the 7 shelf-edge and slope stations in the ECS, the water temperature was higher (26.3-29.3^{o} C) in the surface (≤10 m) and decreased rapidly with depth at all stations (Fig. 2a). In general, for the four shallow stations (Stns. 1, 7, 11 and Z4), the temperature (*T*) were lower than the three slope stations (Z1, Z2 and Z3). The salinity ranged from 33.88 to 34.87 and exhibited opposite profiles from *T* as a reversed *S*-shape: lower in the surface,

Ocean Sci. Discuss., https://doi.org/10.5194/os-2018-78
Manuscript under review for journal Ocean Sci.
Discussion started: 10 September 2018

increasing with depth to 180 m, and decreasing again to 500 m. The salinity (*S*) remained relatively constant below 500 m depth for the three slope stations (Fig. 2b).

For Sta. K2 and the seven deep stations in the KE, temperature (*T*) in the surface water ranged from 14.7 to 24.4° C and exhibited rapid decrease with depth till 1500 m and then remained constant for all stations (Fig. 2c). The largest temperature variations occurred in the upper 700 m with highest *T* (24.4° C) observed at Sta K2 and lowest *T* (14.7° C) at Sta B2 in the surface layer (5 m). Profiles of temperature for the other six stations (Stas. A1-b, A4, A6, A8, B8 and B9) in the KE region showed less variation and decreased similarly from the surface (17.5-20.7° C) to 1500 m (about 2.5° C) and then remained constant in the deeper depth (Fig. 2c). Salinity (*S*) for these stations exhibited higher in the surface and decreased initially to reach minimum, and then increased with depth to about 2500 m (Fig. 2d). The salinity for all stations remained relatively uniform below 2500 m. Like *T*, the largest differences in S profiles also appeared in the upper 700 m water column where low salinity (34.49) was observed in the surface of Sta B2. The salinity decreased to 33.66 around 250 m and then increased to values similar to the other stations at 2500 m. Salinity profiles for the rest seven stations (Stas. K2, A1-b, A4, A6, A8, B8 and B9) showed less variation in surface layers (5m) (34.76 to 34.98), and Sta K2 had the highest *S* (34.98) in the surface among all stations, respectively (Fig. 2d).

3.2 Concentration and distribution of DOC

Concentrations of DOC ranged from 45-88 μM in the ECS and 35-65 μM in the KE region (Fig. 3 and Table S1). As plotted in Fig. 3a, the concentrations of DOC ranged from 55-88 μM for the four shelf-edge stations (Sta. 11, 1, 7 and Z4) and from 45-84 μM for three slope stations (Stas. Z1, Z2 and Z3) in the ECS, respectively. Concentrations of DOC showed fewer variations (71-81 μM) in the surface water among these stations, and decreased nearly parallel with depth down to 45-54 μM at 1000-1400 m depth (Fig. 3a). For stations Stn. 1 and Z1, a DOC sub-maximum in the depth of ~ 50 m was observed.

Ocean Sci. Discuss., https://doi.org/10.5194/os-2018-78
Manuscript under review for journal Ocean Sci.
Discussion started: 10 September 2018

In comparison, the concentrations of DOC in the KE region showed spatial variations (43-65 μM) in the surface water (5 m) with highest value at Sta. B2 and lowest value at Sta. K2, and they decreased with depth even though the trend exhibited some variations among the stations (Fig. 3b). In the upper 200 m depth, concentrations of DOC showed a very rapid decrease from 53 μM to 38 μM at Sta A4. DOC concentrations (36-53 μM) were significantly lower at Sta A4 and Sta B2 than at the other stations in the upper 700 m depth, whereas concentrations were slightly higher in 500 m-800 m depth at Sta B8 and Sta A8. The depth profiles showed that DOC concentrations decreased to much lower levels (36-44 μM) at all stations below 1500 m depth and remained constant in the deep waters (Fig. 3b).

4 Discussion

4.1 Process controlling DOC distribution in the ECS

In this study, the concentrations of DOC measured in the shelf-edge and slope waters are comparable with the values reported previously for the ECS (Hung et al., 2003; Ogawa et al., 2003; Gan et al., 2016). The distribution of DOC in the shelf-edge and slope range of ECS appeared to be primarily controlled by physical processes rather than production and/or microbial processes as manifested by a statistically positive correlation between DOC and water temperature ($R^2 = 0.82$, $p < 0.001$ in Fig. 4a). Similar findings have been obtained by previous studies focused on different regions in the ECS (Hung et al., 2003; Ogawa et al., 2003) and other marginal seas of the NP (Hung et al., 2007; Dai et al., 2009). In our recent study, we have reported that the depth concentrations of DIC and Δ^{14}C-DIC values in the ECS slope and the KE region showed conservative behavior and could be used as tracers of water mass movement and water parcel homogenization as predicted by the solution mixing model (Ge et al., 2016; Ding et al., 2018). In Fig. 4b, we examined the correlations of DOC and DIC concentrations in the ECS. Overall, the negative relationship between DOC and DIC in the ECS ($R^2 = 0.73$, $p <$

Ocean Sci. Discuss., https://doi.org/10.5194/os-2018-78
Manuscript under review for journal Ocean Sci.
Discussion started: 10 September 2018

242 0.001) further indicated that physical processes (such as horizontal and vertical water mixing)
243 influenced the distribution and variation of DOC in the shelf break and slope region of the ECS.
244 Although river inputs play an important role in the ECS, our sampling stations are not likely
245 affected by freshwater input from the Yangtze River, according to the high salinity without any
246 freshwater dilution signals in Fig. 2b. The DOC depth profiles for the shelf-edge and slope
247 stations as shown in Fig. 3a followed a typical trends as DOC depth profiles observed in open
248 oceans. Around the shelf-edge of ECS, the vigorous exchange between the warm saline
249 Kuroshio and cold fresh continental shelf water masses would largely affect the hydrographical
250 characteristics (Hsueh, 2000). Physical models and chemical tracers have provided clear
251 evidence of the intrusion of upwelled Kuroshio intermediate water (500-800 m) into the ECS
252 shelf region (Yang et al., 2011; Yang et al., 2012; Ge et al., 2016). To further demonstrate the
253 influence of different water masses mixing on the hydrological properties, Figure 5 compared
254 the transectional distributions of density (σ_t), DOC/DIC concentrations and Δ^{14}C-DIC for the
255 seven stations. The transectional distribution of density (σ_t) plot (Fig. 5a) showed the water
256 mass in the studied area is composed of mixed Kuroshio and shelf waters. It appeared likely
257 that the influences of Kuroshio intermediate water (500-800 m) on the bottom water at stations
258 Z4 and Stn. 11, which brought low concentrations of DOC, and high concentrations and low
259 Δ^{14}C values of DIC, and which would dilute DOC concentrations at Stn. 11 and Z4 relative to
260 the slope waters below 100 m depth (Figs. 5b-5d). However, it seemed that this upwelling
261 intrusion had almost no effect on the surface water (<100 m depth) for the shelf stations. As
262 shown in Fig. 5d, the well mixed shelf water could not only contribute to the ^{14}C-depleted DIC
263 signature in the upper 100 m layer at station Z4, but also elevate DOC concentrations, as
264 compared with the DOC levels in the upper waters at the other three slope stations (Stas. Z1,
265 Z2 and Z3) influenced by the Kuroshio Current (Figs. 3b and 5b). The river influence and inner
266 shelf export of DOC appeared to be limited in the deep slope stations. The intrusion of Kuroshio

Ocean Sci. Discuss., https://doi.org/10.5194/os-2018-78
Manuscript under review for journal Ocean Sci.
Discussion started: 10 September 2018

intermediate water could reflect a smaller-scale or eddy effect rather than a large-scale influence beyond Stn. 11 and Z4 (Figs. 5c and 5d) (Ge et al., 2016), and it is therefore that the DOC levels at other two shelf stations (Stn. 1 and Stn. 7) were not decreased significantly below 100 m depth (Fig. 5b). Calculation based on the Δ^{14}C-DIC values showed that about 54-65% of the bottom water in the shelf region was from the intrusion of Kuroshio intermediate water (Ge et al., 2016). If we use the two end-member mixing model as reported by Ge et al. (2016), the conservative concentrations of DOC could then be calculated in the range of 65-68 μM which was slightly higher but comparable with the observed DOC values in the bottom waters at Stn. 11 and Z4 (56-61 μM). The negative values (ΔDOC) between the measured and conservative DOC concentrations could represent the biological consumption effects superimposed on the water physical mixing processes around the shelf-edge and in the slope of ECS.

In addition to DOC analyses, apparent oxygen utilization (AOU) for the ECS stations was determined by subtracting observed dissolved oxygen concentration from its saturated solubility at *in situ* potential temperature and salinity. The statistical correlation plotted in Fig. 6 is used to estimate the relationship between DOC and AOU in the ECS. The linear regression slope value (0.132) we obtained for the seven stations ($R^2 = 0.77$, $p < 0.001$, Fig. 6) and the slope values (0.085 to 0.231) obtained in many coastal studies were all well below the stoichiometric molar ratio predicted from Redfield stoichiometry ($-\Delta C/\Delta O_2=0.72$, (Anderson, 1995)). This suggests that only a small fraction (~18%) of the dissolved oxygen consumption was derived from DOC remineralization in the ECS coastal waters. Previous studies have suggested that the remineralization of sinking POM could also contribute part of the dissolved oxygen consumption in ocean waters (Doval and Hansell, 2000; Hung et al., 2007; Pan et al., 2014). However, an alternative explanation considers the mixing of different water masses rather than remineralization of DOC could be important in controlling the apparent correlation between DOC and AOU in coastal waters (Guo et al., 1994; Thomas et al., 1995). This could

Ocean Sci. Discuss., https://doi.org/10.5194/os-2018-78
Manuscript under review for journal Ocean Sci.
Discussion started: 10 September 2018

292 also be the case in the ECS as well and make a significantly statistical correlation between AOU
293 and temperature ($R^2 = 0.95$, $p < 0.001$). However, this scenario needs to be further evaluated
294 based on more sampling stations and results.

295 **4.2 Process influencing DOC profiles in the Kuroshio Extension**

296 In general, biological and physical processes could combine in controlling DOC profiles in
297 open oceans (Hansell and Waterhouse, 1997; Ogawa et al., 1999; Hansell et al., 2009; Carlson
298 et al., 2010; Bercovici and Hansell, 2016). Attributed to the low concentration of nitrate and
299 silicic acid, primary production during spring was low in the KE region (Nishibe et al., 2015).
300 Moreover, very low levels of available dissolved nitrogen (<4 μM) were observed in the region
301 (unpublished data) during the same cruise in spring (April-May 2015). The relatively lower
302 surface DOC concentrations (average 57±7 μM) could be thus due to the low primary
303 production during sampling in the spring season. Despite the low DOC concentrations in the
304 region, however, we observed the interesting feature of relatively large DOC concentration
305 variations among these stations, especially in the upper 1500 m (Fig. 3b). For example,
306 concentrations of DOC in the upper 100 m depth at Sta B2 and A4 located north of and around
307 the KE were significantly lower (average 43±5 μM), close to the deep water values (ca. 36-44
308 μM, average 39±3 μM), while elevated concentrations of surface DOC (61-65 μM) prevailed
309 at Sta K2 located far south of KE and the other five stations (54-63 μM, Stas A1-b, B8, B9, A6
310 and A8), with values 28% higher than average. In the KE region, primary production is largely
311 affected by advection along the KE meander and differed among representative areas in spring,
312 which is high in the northern edge and around the axis (Nishibe et al., 2015). In addition, surface
313 mooring data from the NOAA Kuroshio Extension Observatory (KEO) indicated that physical
314 processes dominate carbon input to the mixed layer at KEO (Fassbender et al., 2017). We thus
315 speculate that the low DOC levels at Sta B2 and A4 were not likely directly related to the low
316 primary production, and instead, the observed large spatial variations were mainly modulated

Ocean Sci. Discuss., https://doi.org/10.5194/os-2018-78
Manuscript under review for journal Ocean Sci.
Discussion started: 10 September 2018

by the mixing dynamics of different water masses rather than biological processes in the region.

Hydrodynamic controls can be evaluated most directly by comparing DOC concentrations to variables of hydrographic properties. In Figs. 4c and 4d, we examined the correlations of DOC concentrations with water temperature and DIC concentrations in the KE region, respectively. Overall, there is a positive relationship between DOC concentrations and temperature in the KE (Fig. 4c, $R^2 = 0.62$, $p < 0.001$), and a negative correlation between DOC and DIC concentrations (Fig. 4d, $R^2 = 0.51$, $p < 0.001$). These observed correlations of DOC concentrations and hydrographic variables indicate the major role of physical water mixing affecting the DOC distribution in the KE region in the northwestern NP. In order to examine the distribution of DOC with different water masses in the KE region, we plotted DOC and DIC concentrations and Δ^{14}C-DIC values superimposed on the plots of potential temperature (θ) and salinity in Fig. 7. It can be seen that the distributions of both DOC, DIC and Δ^{14}C-DIC were clearly associated with different water masses as identified by the potential water density (σ_0). Higher levels of DOC were associated with lower DIC concentrations and high Δ^{14}C-DIC values presented in lower density waters ($\sigma_0 < 25.5$, water mass A), while lower levels of DOC were associated with higher DIC concentrations and low Δ^{14}C-DIC values presented in denser waters ($\sigma_0 > 27.0$, water mass C) (Fig. 7). The denser water mass likely originated from the subarctic gyre which had low temperature and salinity; and were transported by the south-flowing Oyashio Current along the western boundary to the KE region. The lower density water mass with high temperature and salinity, however, were transported by the northeast-flowing Kuroshio Current and mixed with Oyashio Current in the KE region (Figs. 2c and 2d).

Many results suggested that the hydrodynamic process such as the deep vertical convection possibly affected the DOC accumulation within the surface waters in the high latitude, despite high primary production (Ogawa et al., 1999; Ogawa and Tanoue, 2003). Considering the relatively lower temperature (< 15° C) and salinity (< 34.5) in the upper 700 m (Figs. 2c and

Ocean Sci. Discuss., https://doi.org/10.5194/os-2018-78
Manuscript under review for journal Ocean Sci.
Discussion started: 10 September 2018

2d), Sta B2 was mainly affected by the intrusion of cold and fresh subarctic water transported by the southward-flowing Oyashio which also carried lower concentrations of DOC. In contrast, in spite of nutrient-depleted and low primary productivity in the subtropical gyre, the physical stability such as the water column stratification could restrict the vertical mixing of the surface and deep water, which provided environments for DOC accumulation in the surface layer. The relatively higher DOC level in the upper 200 m at Sta K2 was influenced by the northeastward-flowing Kuroshio, which carries a subtropical warm, high-salinity water mass in upper layers as demonstrated in Figs. 2c and 2d. Hydrographic properties and DOC profiles of the other five stations (A1-b, B8, B9, A6 and A8) in the KE region showed similar patterns with Sta K2, suggesting that the Kuroshio water dominated the mixing at these stations. This can be demonstrated more clearly in Fig. 8 when we plotted the salinity, DOC and DIC concentrations and Δ^{14}C-DIC values for the five stations (B2, A4, A1-b, B8 and B9) as a cross KE transect from north to south. It can be seen that the Kuroshio, which carries relatively high DOC, dominated stations B9, B8 and A1-b from ~ 200-1500 m depth. The Oyashio, on the other hand, carrying low salinity, low DOC but high DIC concentrations, and low Δ^{14}C-DIC values subarctic intermediate water, influenced the entire water column at Sta B2 and intruded upward affecting the upper 100-700 m water column of Sta A4, and mixed with the Kuroshio water to form the KE water mass. The unstable mode of the KE could generate active water-mass changes between the south and the north of the KE, thus enhancing meso-scale eddy activities and allowing ocean recirculation formation around the region (Qiu and Chen, 2005; Qiu and Chen, 2011; Ma et al., 2016). This unstable KE mode could transport the fresher Oyashio-origin water southward through meso-scale eddies (Qiu and Chen, 2011), influencing the chemical and biological processes in the KE region. Using dissolved inorganic radiocarbon measurements (Δ^{14}C-DIC), we also demonstrated the same strong influence of the southward Oyashio-transported subarctic intermediate water mass via meso-scale eddies, which cause the

Ocean Sci. Discuss., https://doi.org/10.5194/os-2018-78
Manuscript under review for journal Ocean Sci.
Discussion started: 10 September 2018

significantly low Δ^{14}C-DIC values at stations B2 and A4 in the upper 700 m depth (Ding et al., 2018). The ratios of Oyashio water to Kuroshio water mixing for the five stations (B2, B8, A4, A8 and B9) were obtained by mass balance calculations based on the selected two end-member Δ^{14}C-DIC values in the Δ^{14}C-DIC Keeling plot analysis (Fig. 9) (Ding et al., 2018). If we considered the distribution of DOC is controlled mainly by hydrodynamic mixing in the KE region, the conservative concentrations of DOC could then be calculated by using the two water masses mixing model derived from the Δ^{14}C-DIC values, within the range of 40-56 μM. The difference between the measured and conservative DOC concentrations (ΔDOC) represent other biological processes secondly modulated DOC in the KE region. For example, positive ΔDOC values (~ 6 μM) at Sta B8 indicated net DOC increase from biological processes, accompanying with relative low DIC concentrations shown in Fig. 8c. The recirculation gyre just south of the KE has been found to exhibit some of high production rates in winter-spring season in the North Pacific due to the entrainment of nutrient-rich water during deep winter mixing (Yasunaka et al., 2013; Yasunaka et al., 2014).

Concentrations of DOC in deep waters in the KE region were low, in the range of 36-44 μM, comparable with the values reported for the deep North Pacific (Druffel et al., 1992; Hansell and Carlson, 1998; Hansell et al., 2009) and the deep South Pacific (34-43 μM) (Doval and Hansell, 2000; Druffel and Griffin, 2015), but slightly lower than the values in the North Atlantic (40-48 μM) (Carlson et al., 2010; Druffel et al., 2016). These uniformly low levels of DOC indicate the homogeneity distribution of deep water and the more presumably refractory DOC left behind in deeper waters in the KE and North Pacific (Carlson et al., 2010; Hansell et al., 2012; Follett et al., 2014). Radiocarbon measurements of DOC collected in the KE indicate that the ^{14}C ages of DOC in the deep water was ~ 6,200 years old (Wang, unpublished data), similar to the DOC ages in the deep NP (Druffel et al., 1992) and support the refractory nature of DOC in the deep KE. The lower deep DOC concentrations in the North Pacific relative to

Ocean Sci. Discuss., https://doi.org/10.5194/os-2018-78
Manuscript under review for journal Ocean Sci.
Discussion started: 10 September 2018

the North Atlantic could be due to the differences in thermohaline circulation patterns as proposed by Hansell et al. (1998), which presented changes in the deep-ocean DOC concentrations along the abyssal circulation pathway.

5 Summary

The results of our study indicate that the concentration of DOC ranged from 45-88 μM in the outer shelf and slope range of ECS and 35-65 μM in the KE region. The distribution of DOC in the shelf-edge and slope range of the ECS was largely controlled by physical mixing processes of Kuroshio and ECS shelf waters. The upwelling intrusion of Kuroshio intermediate water could dilute the DOC concentrations at stations around the shelf break region of the ECS. The inversely correlated DOC and AOU suggested that DOC oxidation only contributed 18% of the oxygen consumption in the water column, and the distributions of DOC and AOU were both mainly controlled by the physical process in the slope waters of the ECS.

In comparison, concentrations of DOC in the KE region were significantly lower in the surface layer. DOC in the deep water of the KE had similar and comparable values as reported for the deep north and south Pacific. The large spatial variations of DOC in the upper 700 m among the stations in the KE were influenced mainly by the hydrodynamic mixing of two different water masses. The Kuroshio which carries warm and relatively higher DOC, and the Oyashio which carries cold and fresh subarctic intermediate water with lower DOC, mix to form KE. This mixing dynamics could have a major influence not only on primary production but biogeochemical processes as well in the KE region.

Data availability. All data used in this study will be freely available, for scientific use only, upon request. Anyone interested in using this data set for scientific research should contact the

417 corresponding author via e-mail.
418
419
420

421 *Author contributions.* Ling Ding is a post-doc working on this project, participated in the cruises,
422 sample analysis and manuscript writing. Tiantian Ge is a laboratory technician participated in
423 all cruises, sampling and sample analysis. Dr. Xuchen Wang is the corresponding author and
424 leading scientist for this study from proposal writing, cruise and sampling planning, and
425 manuscript writing. All authors have read the manuscript and agreed on the authorship.
426
427
428

429 *Competing interests.* The authors declare that they have no conflict of interest.
430
431
432

433 *Acknowledgments.* We thank Drs. Lixin Wu and Jing Zhang for providing the ECS and KE
434 cruise opportunity and Drs. Huiwang Gao and Lei Li for the help during sample collection. We
435 thank Yuejun Xue, Chunle Luo, Caili Xu, Yuanzhi Qi and Sen Shan for help and assistance
436 during sample analysis in laboratory. We give our special thanks to the Captains and crew
437 members of *R/V Dongfanghong-2* and *R/V Shinset Maru* for help during the cruises. Financial
438 support for this work was provided by the National Natural Science Foundation of China (grant
439 numbers: 91428101 and 41476057) and the Fundamental Research Funds for the Central
440 Universities (grant number: 201762009).
441
442
443

444 **References**

445 Abell, J., Emerson, S. and Renaud, P.: Distributions of TOP, TON and TOC in the North Pacific
446 subtropical gyre: Implications for nutrient supply in the surface ocean and remineralization in the
447 upper thermocline, J. Mar. Res., 58, 203-222, http://doi.org/10.1357/002224000321511142, 2000.
448 Anderson, L. A.: On the hydrogen and oxygen content of marine phytoplankton, Deep-Sea Res. Pt. I,
449 42, 1675-1680, http://doi.org/10.1016/0967-0637(95)00072-E, 1995.

450 Azam, F., Fenchel, T., Field, J. G., Gray, J., Meyer-Reil, L. and Thingstad, F.: The ecological role of
451 water-column microbes in the sea, Mar. Ecol Prog Ser., 20, 257-263, 1983.
452 Bercovici, S. K. and Hansell, D. A.: Dissolved organic carbon in the deep Southern Ocean: Local versus
453 distant controls, Global Biogeochem. Cycles, 30, 350-360, http://doi.org/10.1002/2015GB005252,
454 2016.
455 Carlson, C. A., Ducklow, H. W., Hansell, D. A. and Smith, W. O.: Organic carbon partitioning during
456 spring phytoplankton blooms in the Ross Sea polynya and the Sargasso Sea, Limnol. Oceanogr., 43,
457 375-386, http://doi.org/10.4319/lo.1998.43.3.0375, 1998.
458 Carlson, C. A., Ducklow, H. W. and Michaels, A. F.: Annual flux of dissolved organic carbon from the
459 euphotic zone in the northwestern Sargasso Sea, Nature, 371, 405-408, http://doi.org/10.1038/371405
460 a0, 1994.
461 Carlson, C. A., Hansell, D. A., Nelson, N. B., Siegel, D. A., Smethie, W. M., Khatiwala, S., Meyers, M.
462 M. and Halewood, E.: Dissolved organic carbon export and subsequent remineralization in the
463 mesopelagic and bathypelagic realms of the North Atlantic basin, Deep-Sea Res. Pt. II, 57, 1433-
464 1445, http://doi.org/10.1016/j.dsr2.2010.02.013, 2010.
465 Chen, C.-T. A. and Wang, S.-L.: Carbon, alkalinity and nutrient budgets on the East China Sea
466 continental shelf, J. Geophys. Res.: Oceans, 104, 20675-20686, http://doi.org/10.1029/1999jc900055,
467 1999.
468 Dai, M., Meng, F., Tang, T., Kao, S.-J., Lin, J., Chen, J., Huang, J.-C., Tian, J., Gan, J. and Yang, S.:
469 Excess total organic carbon in the intermediate water of the South China Sea and its export to the
470 North Pacific, Geochem. Geophys. Geosyst., 10, Q12002, http://doi.org/10.1029/2009GC002752,
471 2009.
472 Ding, L., Ge, T., Gao, H., Luo, C., Xue, Y., Druffel, E. R. M. and Wang, X.: Large variability of dissolved
473 inorganic radiocarbon in the Kuroshio Extension of the northwest North Pacific, Radiocarbon, 60,
474 691-704, http://doi.org/10.1017/RDC.2017.143, 2018.
475 Doval, M. D. and Hansell, D. A.: Organic carbon and apparent oxygen utilization in the western South
476 Pacific and the central Indian Oceans, Mar. Chem., 68, 249-264, http://doi.org/10.1016/S0304-
477 4203(99)00081-X, 2000.
478 Druffel, E. R., Williams, P. M., Bauer, J. E. and Ertel, J. R.: Cycling of dissolved and particulate organic
479 matter in the open ocean, J. Geophys. Res., 97, 15639-15659, 1992.
480 Druffel, E. R. M. and Griffin, S.: Radiocarbon in dissolved organic carbon of the South Pacific Ocean,
481 Geophys. Res. Lett., 42, 4096-4101, http://doi.org/10.1002/2015GL063764, 2015.
482 Druffel, E. R. M., Griffin, S., Coppola, A. I. and Walker, B. D.: Radiocarbon in dissolved organic carbon
483 of the Atlantic Ocean, Geophys. Res. Lett., 43, 5279-5286, http://doi.org/10.1002/2016GL068746,
484 2016.
485 Fassbender, A. J., Sabine, C. L., Cronin, M. F. and Sutton, A. J.: Mixed-layer carbon cycling at the
486 Kuroshio Extension Observatory, Global Biogeochem. Cycles, 31, 272-288, http://doi.org/10.1002/
487 2016GB005547, 2017.
488 Fenchel, T.: The microbial loop-25 years later, J. Exp. Mar. Bio. Ecol., 366, 99-103, http://doi.org/10.
489 1016/j.jembe.2008.07.013, 2008.
490 Follett, C. L., Repeta, D. J., Rothman, D. H., Xu, L. and Santinelli, C.: Hidden cycle of dissolved organic
491 carbon in the deep ocean, Proc. Natl. Acad. Sci. USA., 111, 16706-16711, http://doi.org/10. 1073/
492 pnas.1407445111, 2014.
493 Gan, S., Wu, Y. and Zhang, J.: Bioavailability of dissolved organic carbon linked with the regional
494 carbon cycle in the East China Sea, Deep-Sea Res. Pt. II, 124, 19-28, http://doi.org/10.1016/j.dsr2.
495 2015.06.024, 2016.

496 Ge, T., Wang, X., Zhang, J., Luo, C. and Xue, Y.: Dissolved inorganic radiocarbon in the Northwest
497 Pacific continental margin, Radiocarbon, 58, 517-529, http://doi.org/10.1017/RDC.2016.23, 2016.
498 Gong, G.-C., Wen, Y.-H., Wang, B.-W. and Liu, G.-J.: Seasonal variation of chlorophyll a concentration,
499 primary production and environmental conditions in the subtropical East China Sea, Deep-Sea Res.
500 Pt. II, 50, 1219-1236, http://doi.org/10.1016/S0967-0645(03)00019-5, 2003.
501 Guo, L., Coleman, C. H. and Santschi, P. H.: The distribution of colloidal and dissolved organic carbon
502 in the Gulf of Mexico, Mar. Chem., 45, 105-119, http://doi.org/10.1016/0304-4203(94)90095-7, 1994.
503 Guo, X., Miyazawa, Y. and Yamagata, T.: The Kuroshio onshore intrusion along the shelf break of the
504 East China Sea: The origin of the Tsushima Warm Current, J. Phys. Oceanogr., 36, 2205-2231,
505 http://doi.org/10.1175/JPO2976.1, 2006.
506 Hansell, D. A. and Carlson, C. A.: Deep-ocean gradients in the concentration of dissolved organic carbon,
507 Nature, 395, 263-266, http://doi.org/10.1038/26200, 1998.
508 Hansell, D. A. and Carlson, C. A.: Marine dissolved organic matter and the carbon cycle, Oceanography,
509 14, 41-49, 2001.
510 Hansell, D. A., Carlson, C. A., Repeta, D. J. and Schlitzer, R.: Dissolved organic matter in the ocean: A
511 controversy stimulates new insights, Oceanography, 22, 202-211, http://doi.org/10.5670/oceanog.
512 2009.109, 2009.
513 Hansell, D. A., Carlson, C. A. and Schlitzer, R.: Net removal of major marine dissolved organic carbon
514 fractions in the subsurface ocean, Global Biogeochem. Cycles, 26, GB1016, http://doi.org/10.1029/
515 2011gb004069, 2012.
516 Hansell, D. A., Carlson, C. A. and Suzuki, Y.: Dissolved organic carbon export with North Pacific
517 Intermediate Water formation, Global Biogeochem. Cycles, 16, 1007, http://doi.org/10.1029/2000
518 GB001361, 2002.
519 Hansell, D. A. and Waterhouse, T. Y.: Controls on the distributions of organic carbon and nitrogen in the
520 eastern Pacific Ocean, Deep-Sea Res. Pt. I, 44, 843-857, http://doi.org/10.1016/S0967-0637(96)
521 00128-8, 1997.
522 Hsueh, Y.: The Kuroshio in the East China Sea, J. Mar. Syst., 24, 131-139, http://doi.org/10.1016/S0924-
523 7963(99)00083-4, 2000.
524 Hu, D., Wu, L., Cai, W., Gupta, A. S., Ganachaud, A., Qiu, B., Gordon, A. L., Lin, X., Chen, Z., Hu, S.,
525 Wang, G., Wang, Q., Sprintall, J., Qu, T., Kashino, Y., Wang, F. and Kessler, W. S.: Pacific western
526 boundary currents and their roles in climate, Nature, 522, 299-308, http://doi.org/10.1038/nature
527 14504, 2015.
528 Hung, J. J., Chen, C. H., Gong, G. C., Sheu, D. D. and Shiah, F. K.: Distributions, stoichiometric patterns
529 and cross-shelf exports of dissolved organic matter in the East China Sea, Deep-Sea Res. Pt. II, 50,
530 1127-1145, http://doi.org/10.1016/S0967-0645(03)00014-6, 2003.
531 Hung, J. J., Wang, S. M. and Chen, Y. L.: Biogeochemical controls on distributions and fluxes of
532 dissolved and particulate organic carbon in the Northern South China Sea, Deep-Sea Res. Pt. II, 54,
533 1486-1503, http://doi.org/10.1016/j.dsr2.2007.05.006, 2007.
534 Ma, X., Zhao, J., Chang, P., Liu, X., Montuoro, R., Small, R. J., Bryan, F. O., Greatbatch, R. J., Brandt,
535 P., Wu, D., Lin, X. and Wu, L.: Western boundary currents regulated by interaction between ocean
536 eddies and the atmosphere, Nature, 535, 533-537, http://doi.org/10.1038/nature18640, 2016.
537 McNichol, A. P., Jones, G. A., Hutton, D. L., Gagnon, A. R. and Key, R. M.: The rapid preparation of
538 seawater $\sum CO_2$ for radiocarbon analysis at the National Ocean Sciences AMS Facility, Radiocarbon,
539 36, 237-246, 1994.
540 Nelson, C. E. and Carlson, C. A.: Tracking differential incorporation of dissolved organic carbon types
541 among diverse lineages of Sargasso Sea bacterioplankton, Environ Microbiol., 14, 1500-1516,

http://doi.org/10.1111/j.1462-2920.2012.02738.x, 2012.

Nishibe, Y., Takahashi, K., Sato, M., Kodama, T., Kakehi, S., Saito, H. and Furuya, K.: Phytoplankton community structure, as derived from pigment signatures, in the Kuroshio Extension and adjacent regions in winter and spring, J Oceanogr., 73, 463-478, http://doi.org/10.1007/s10872-017-0415-3, 2017.

Nishibe, Y., Takahashi, K., Shiozaki, T., Kakehi, S., Saito, H. and Furuya, K.: Size-fractionated primary production in the Kuroshio Extension and adjacent regions in spring, J Oceanogr., 71, 27-40, http://doi.org/10.1007/s10872-014-0258-0, 2015.

Ogawa, H., Fukuda, R. and Koike, I.: Vertical distributions of dissolved organic carbon and nitrogen in the Southern Ocean, Deep-Sea Res. Pt. I, 46, 1809-1826, http://doi.org/10.1016/S0967-0637(99)00027-8, 1999.

Ogawa, H. and Tanoue, E.: Dissolved Organic Matter in oceanic waters, J Oceanogr., 59, 129-147, http://doi.org/10.1023/a:1025528919771, 2003.

Ogawa, H., Usui, T. and Koike, I.: Distribution of dissolved organic carbon in the East China Sea, Deep-Sea Res. Pt. II, 50, 353-366, http://doi.org/10.1016/S0967-0645(02)00459-9, 2003.

Pan, X., Achterberg, E. P., Sanders, R., Poulton, A. J., Oliver, K. I. C. and Robinson, C.: Dissolved organic carbon and apparent oxygen utilization in the Atlantic Ocean, Deep-Sea Res. Pt. I, 85, 80-87, http://doi.org/10.1016/j.dsr.2013.12.003, 2014.

Qiu, B.: Kuroshio and Oyashio currents, in: Encyclopedia of Ocean Science, edited by: Steele, J. H., Turekian, K. K. and Thorpe, S. A., 1413–1425, Academic Press, San Diego, 2001.

Qiu, B. and Chen, S.: Variability of the Kuroshio Extension Jet, recirculation gyre, and mesoscale eddies on decadal time scales, J. Phys. Oceanogr., 35, 2090-2103, http://doi.org/10.1175/jpo2807.1, 2005.

Qiu, B. and Chen, S.: Effect of decadal Kuroshio Extension Jet and eddy variability on the modification of North Pacific Intermediate Water, J. Phys. Oceanogr., 41, 503-515, http://doi.org/10.1175/2010JPO4575.1, 2011.

Riedel, T. and Dittmar, T.: A method detection limit for the analysis of natural organic matter via Fourier Transform Ion Cyclotron Resonance Mass Spectrometry, Anal Chem., 86, 8376-8382, http://doi.org/10.1021/ac501946m, 2014.

Sharp, J. H., Benner, R., Bennett, L., Carlson, C. A., Fitzwater, S. E., Peltzer, E. T. and Tupas, L. M.: Analyses of dissolved organic carbon in seawater: the JGOFS EqPac methods comparison, Mar. Chem., 48, 91-108, http://doi.org/10.1016/0304-4203(94)00040-K, 1995.

Sharp, J. H., Carlson, C. A., Peltzer, E. T., Castle-Ward, D. M., Savidge, K. B. and Rinker, K. R.: Final dissolved organic carbon broad community intercalibration and preliminary use of DOC reference materials, Mar. Chem., 77, 239-253, http://doi.org/10.1016/S0304-4203(02)00002-6, 2002.

Stuiver, M. and Polach, H. A.: Discussion reporting of ^{14}C data, Radiocarbon, 19, 355-363, http://doi.org/10.1017/S0033822200003672, 1977.

Talley, L. D.: Distribution and formation of North Pacific Intermediate Water, J. Phys. Oceanogr., 23, 517-537, http://doi.org/10.1175/1520-0485(1993)023<0517:dafonp>2.0.co;2, 1993.

Talley, L. D.: North Pacific Intermediate Water transports in the mixed water region, J. Phys. Oceanogr., 27, 1795-1803, http://doi.org/10.1175/1520-0485(1997)027<1795:npiwti>2.0.co;2, 1997.

Thomas, C., Cauwet, G. and Minster, J.-F.: Dissolved organic carbon in the equatorial Atlantic Ocean, Mar. Chem., 49, 155-169, http://doi.org/10.1016/0304-4203(94)00061-H, 1995.

Tsunogai, S., Ono, T. and Watanabe, S.: Increase in total carbonate in the western North Pacific water and a hypothesis on the missing sink of anthropogenic carbon, J Oceanogr., 49, 305-315, http://doi.org/10.1007/bf02269568, 1993.

Wang, X., Ma, H., Li, R., Song, Z. and Wu, J.: Seasonal fluxes and source variation of organic carbon

588 transported by two major Chinese Rivers: The Yellow River and Changjiang (Yangtze) River, Global
589 Biogeochem. Cycles, 26, GB2025, http://doi.org/10.1029/2011GB004130, 2012.
590 Wu, L., Cai, W., Zhang, L., Nakamura, H., Timmermann, A., Joyce, T., McPhaden, M. J., Alexander,
591 M., Qiu, B., Visbeck, M., Chang, P. and Giese, B.: Enhanced warming over the global subtropical
592 western boundary currents, Nat. Clim. Change, 2, 161-166, http://doi.org/10.1038/nclimate1353,
593 2012.
594 Xu, C., Xue, Y., Qi, Y. and Wang, X.: Quantities and fluxes of dissolved and particulate black carbon in
595 the Changjiang and Huanghe Rivers, China, Estuar Coast., 39, 1617-1625, http://doi.org/10.1007/
596 s12237-016-0122-0, 2016.
597 Yang, D., Yin, B., Liu, Z., Bai, T., Qi, J. and Chen, H.: Numerical study on the pattern and origins of
598 Kuroshio branches in the bottom water of southern East China Sea in summer, J. Geophys. Res.:
599 Oceans, 117, C02014, http://doi.org/10.1029/2011JC007528, 2012.
600 Yang, D., Yin, B., Liu, Z. and Feng, X.: Numerical study of the ocean circulation on the East China Sea
601 shelf and a Kuroshio bottom branch northeast of Taiwan in summer, J. Geophys. Res.: Oceans, 116,
602 C05015, http://doi.org/10.1029/2010JC006777, 2011.
603 Yasuda, I.: Hydrographic structure and variability in the Kuroshio-Oyashio transition area, J Oceanogr.,
604 59, 389-402, http://doi.org/10.1023/a:1025580313836, 2003.
605 Yasuda, I., Okuda, K. and Shimizu, Y.: Distribution and modification of North Pacific Intermediate
606 Water in the Kuroshio-Oyashio interfrontal zone, J. Phys. Oceanogr., 26, 448-465, http://doi.org/
607 10.1175/1520-0485(1996)026<0448:damonp>2.0.co;2, 1996.
608 Yasunaka, S., Nojiri, Y., Nakaoka, S.-i., Ono, T., Mukai, H. and Usui, N.: Monthly maps of sea surface
609 dissolved inorganic carbon in the North Pacific: Basin-wide distribution and seasonal variation, J.
610 Geophys. Res.: Oceans, 118, 3843-3850, http://doi.org/10.1002/jgrc.20279, 2013.
611 Yasunaka, S., Nojiri, Y., Nakaoka, S.-i., Ono, T., Whitney, F. A. and Telszewski, M.: Mapping of sea
612 surface nutrients in the North Pacific: Basin-wide distribution and seasonal to interannual variability,
613 J. Geophys. Res.: Oceans, 119, 7756-7771, http://doi.org/10.1002/2014JC010318, 2014.
614
615
616
617

Ocean Sci. Discuss., https://doi.org/10.5194/os-2018-78
Manuscript under review for journal Ocean Sci.
Discussion started: 10 September 2018

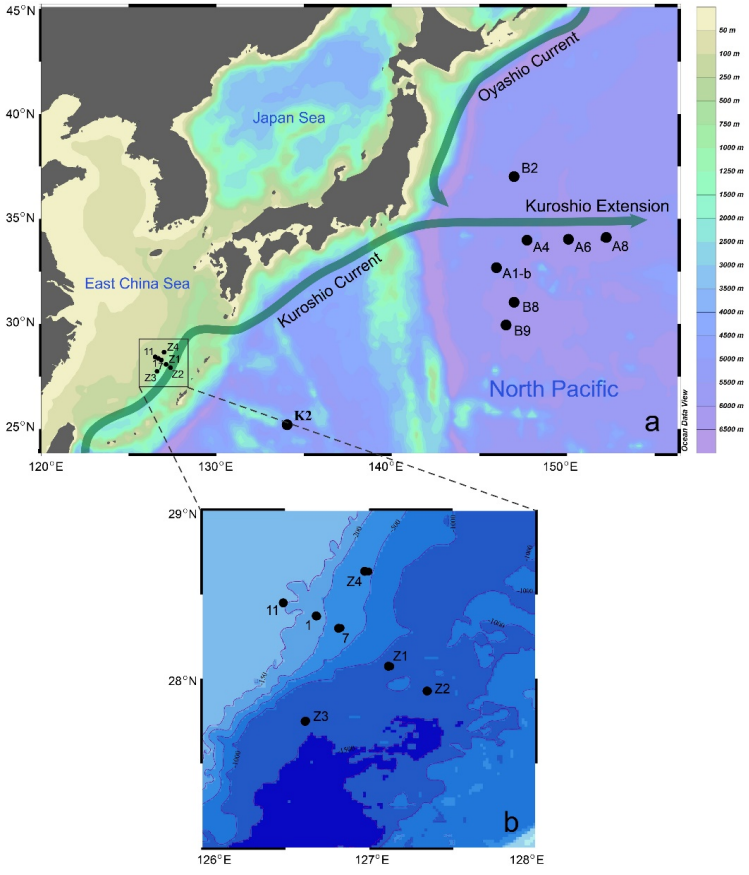

Figure 1. Map showing the study region and the sampling stations in the ECS and in the northwestern North Pacific (NP) during two cruises in 2014-2015 described in the text. Two major western boundary currents, the northeastward-flowing Kuroshio and southward- flowing Oyashio, meet and form the Kuroshio Extension (KE) flowing eastward to the North Central Pacific (NCP).

Ocean Sci. Discuss., https://doi.org/10.5194/os-2018-78
Manuscript under review for journal Ocean Sci.
Discussion started: 10 September 2018

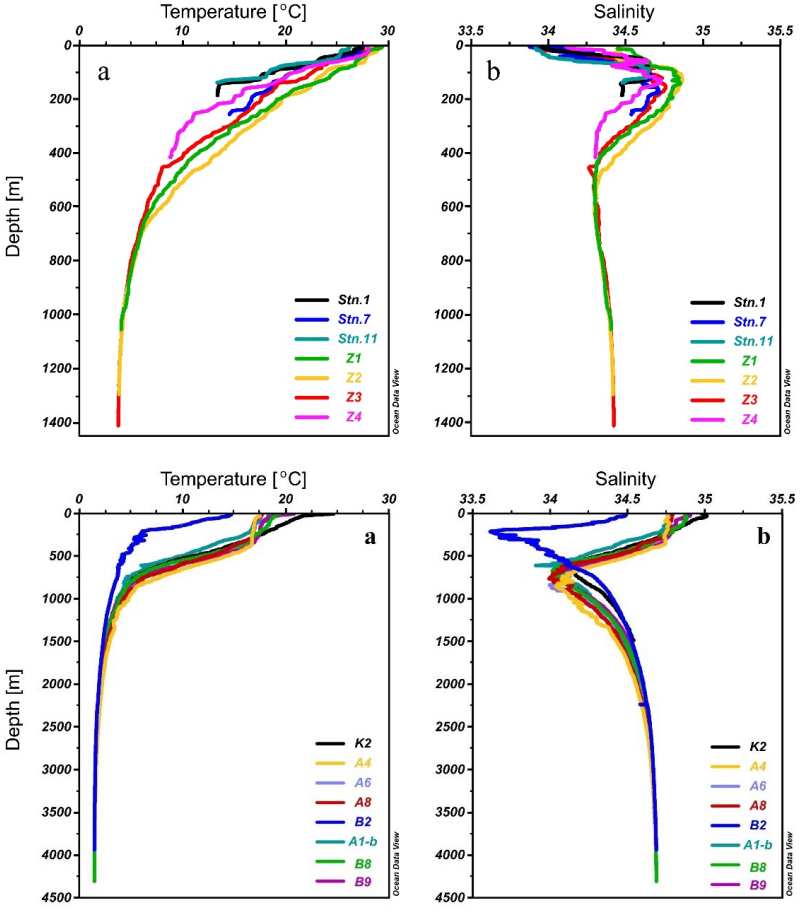

Figure 2. Water temperature and salinity profiles for the stations studied. (a, b) seven shelf to slope stations in the ECS; (c, d) eight deep stations in the northwestern NP.

Ocean Sci. Discuss., https://doi.org/10.5194/os-2018-78
Manuscript under review for journal Ocean Sci.
Discussion started: 10 September 2018

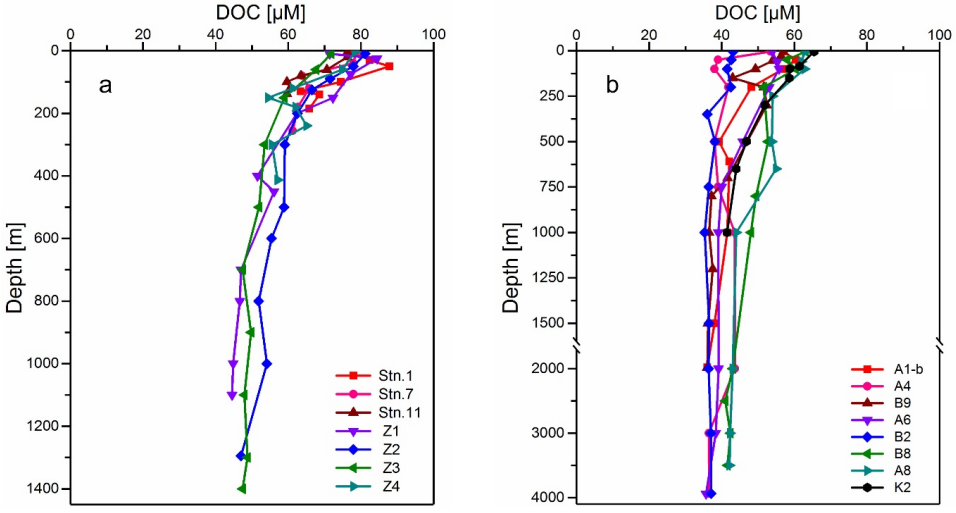

Figure 3. Depth profiles of DOC concentrations measured for the stations (a) in the ECS and (b) in the northwestern NP during the two cruises in 2014-2015. Note: the depth scale below 1500 m has been reduced in (b).

Ocean Sci. Discuss., https://doi.org/10.5194/os-2018-78
Manuscript under review for journal Ocean Sci.
Discussion started: 10 September 2018

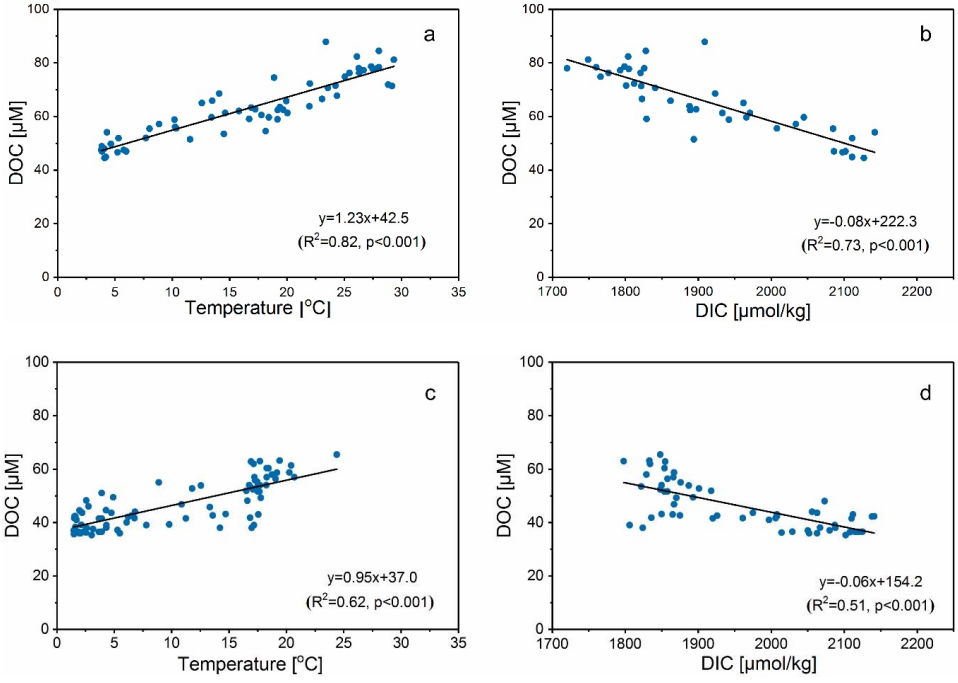

Figure 4. Correlation of DOC concentrations with water temperature and DIC concentrations for stations sampled in (a, b) the ECS and (c, d) the KE. The solid lines are linear regressions fit to the data.

Ocean Sci. Discuss., https://doi.org/10.5194/os-2018-78
Manuscript under review for journal Ocean Sci.
Discussion started: 10 September 2018

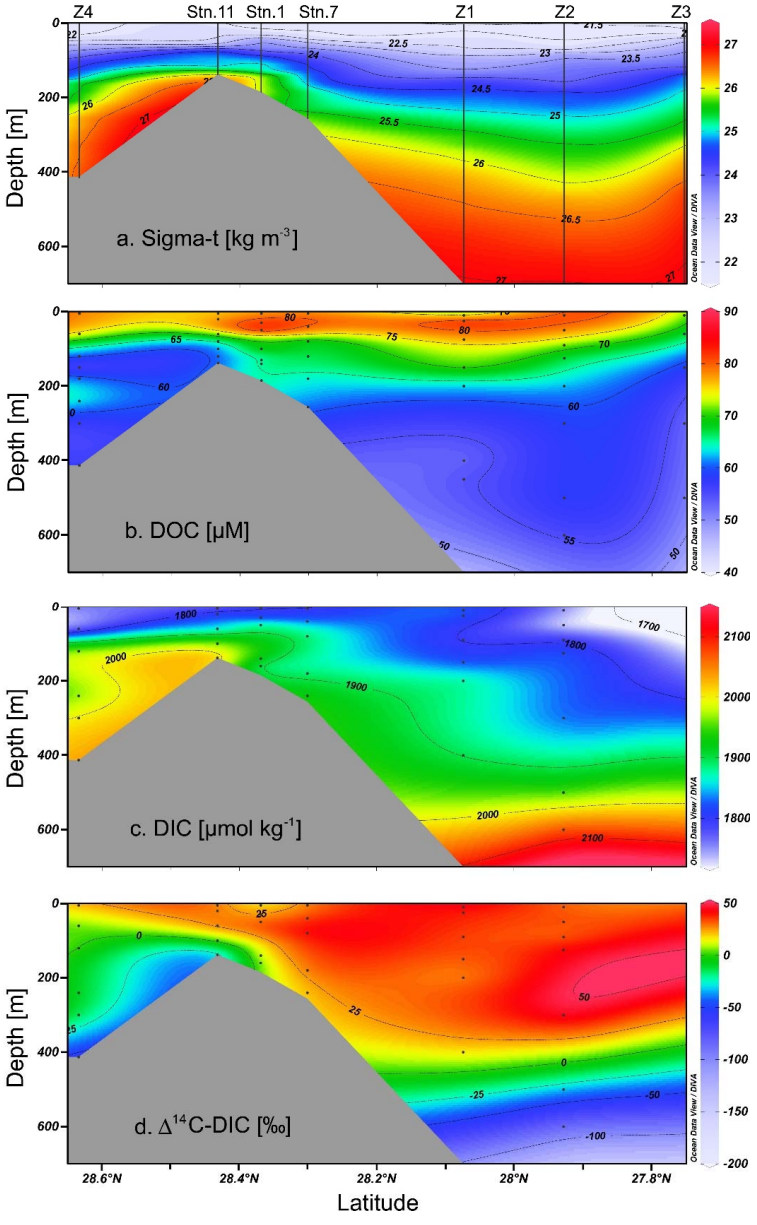

Figure 5. Transectional distributions of (a) density (Sigma-t, σ_t), (b) DOC concentrations, (c) DIC concentrations and (d) Δ^{14}C-DIC values for the sampling stations covered the shelf-edge and slope range of ECS during the cruise in July 2014. Black dots indicate depths where samples were collected. Note: Distributions of density and DOC concentrations include seven stations, whereas DIC concentrations and Δ^{14}C-DIC values were only for six stations due to the lack of data at Sta. Z3 (Ge et al., 2016).

Ocean Sci. Discuss., https://doi.org/10.5194/os-2018-78
Manuscript under review for journal Ocean Sci.
Discussion started: 10 September 2018

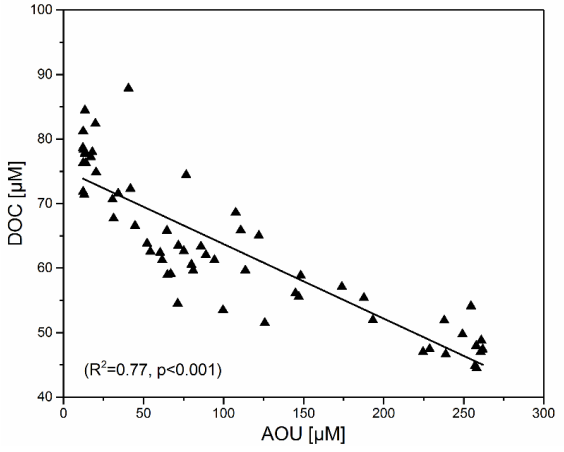

Figure 6. Plot of concentrations of DOC *vs*. AOU (apparent oxygen utilization) for stations in the ECS. Solid line represents the least-squares fit to the data. The generated Model II geometric mean regressions (slope) for the stations were given in the main text.

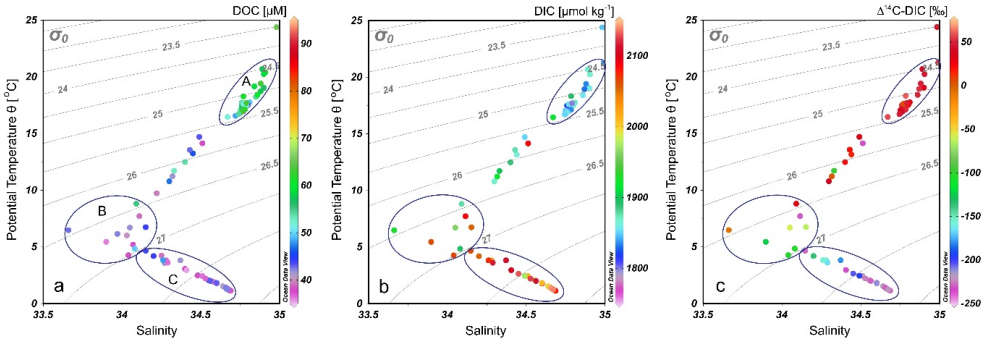

Figure 7. Plot potential temperature (θ) *vs.* salinity with (a) DOC concentrations, (b) DIC concentrations and (c) Δ^{14}C-DIC values (indicated as the colors of points) associated with the potential water density (σ_0) for eight stations in the northwestern North Pacific (NP). The circular areas represented different water masses as (A) lower density water in the upper 300 m depth with higher DOC concentration, lower DIC concentration and enriched Δ^{14}C-DIC; (B) mixed intermediated water in 500-800 m water depth; and (C) denser NP deep water below 1000 m depth. Note: DOC concentrations were measured for all stations, whereas DIC results from Ding et al. (2018) were only measured for six stations except Stas. A1-b and A6.

Ocean Sci. Discuss., https://doi.org/10.5194/os-2018-78
Manuscript under review for journal Ocean Sci.
Discussion started: 10 September 2018

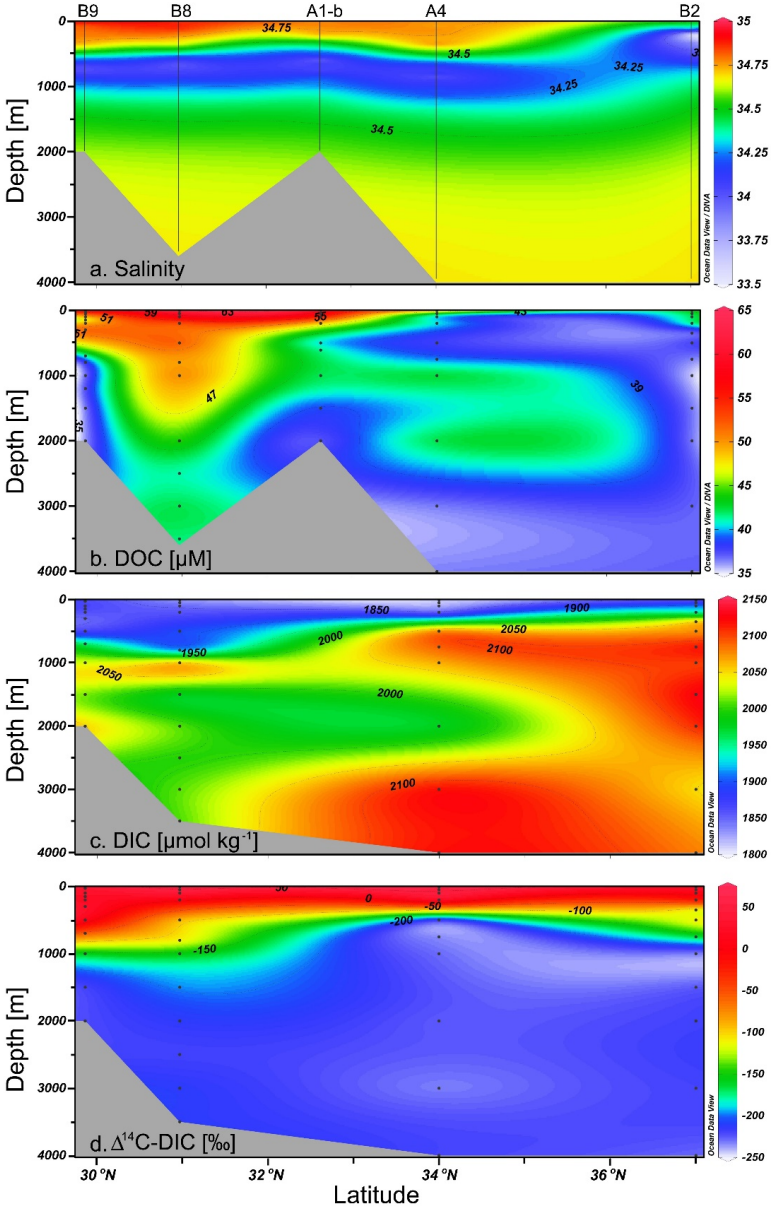

669

670 **Figure 8.** Transectional distributions of (a) salinity, (b) DOC concentrations, (c) DIC
671 concentration and (d) Δ^{14}C-DIC values for stations sampled cross the Kuroshio Extension (KE)
672 in the northwestern NP. Black dots indicate depths where samples were collected. Note: Salinity
673 and DOC concentrations were measured for five stations (B9, B8, A1-b, A4 and B2), whereas
674 DIC concentrations and Δ^{14}C-DIC values were only for four stations due to the lack of data at
675 Sta. A1-b (Ding et al., 2018).

Ocean Sci. Discuss., https://doi.org/10.5194/os-2018-78
Manuscript under review for journal Ocean Sci.
Discussion started: 10 September 2018

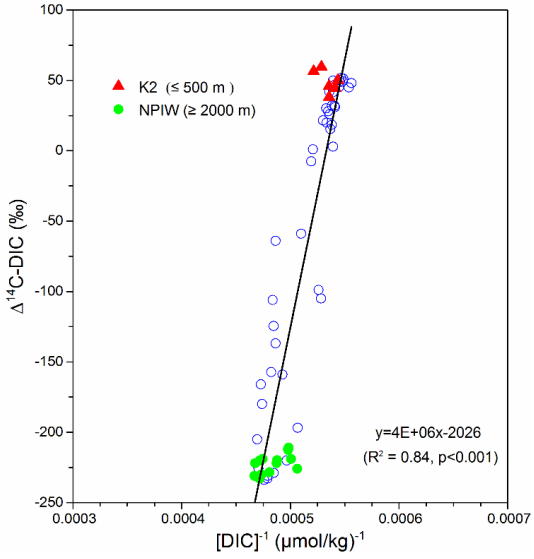

676

677 **Figure 9.** Keeling plot of Δ^{14}C-DIC *vs.* concentration of $[DIC]^{-1}$ measured for six stations (B9,
678 B8, A4, A8, B2 and K2) in the northwestern NP. Red-filled triangles and green-filled circles
679 denote the Kuroshio water and the NPIW of Oyashio mentioned in Ding et al. (2018). The line
680 is the linear regression fit to all data points.

681

682